

Research Article

Gasification Reaction Characteristics between Biochar and CO₂ as well as the Influence on Sintering Process

Min Gan, Wei Lv, Xiaohui Fan, Xuling Chen, Zhiyun Ji, and Tao Jiang

School of Minerals Processing & Bioengineering, Central South University, Changsha, Hunan 410083, China

Correspondence should be addressed to Xiaohui Fan; csufxh@126.com

Received 4 June 2017; Accepted 17 September 2017; Published 23 October 2017

Academic Editor: Merrick Mahoney

Copyright © 2017 Min Gan et al. This is an open access article distributed under the Creative Commons Attribution License, which permits unrestricted use, distribution, and reproduction in any medium, provided the original work is properly cited.

For achieving green production of iron ore sintering, it is significant to substitute biochar, which is a clean and renewable energy, for fossil fuels. In this paper, the gasification reaction between CO₂ and biochar was investigated. The results showed the initial temperature and the final temperature of the gasification reaction between biochar and CO₂ were lower, while the maximum weight loss rate and the biggest heat absorption value were much higher than those of coke breeze, which indicated gasification reaction between the biochar and CO₂ occurred rapidly at lower temperature. The gasification activation energy of biochar was 131.10 kJ/mol, which was lower than that of the coke breeze by 56.26 kJ/mol. Therefore, biochar had a higher reactivity and easily reacted with CO₂ to generate CO. As a result, when biochar replaced coke powder at equal heat condition in sintering process, the combustion efficiency of fuel decreased and was disadvantage to the mineralization of iron ores at high temperature. With the increase of substitute proportion, the sinter yield, tumble strength, and productivity were decreased. The proportion of biochar replacing coke breeze should not be higher than 40%. By reducing the heat replacement ratio of biochar, the yield and quality of sinter got improved.

1. Introduction

The energy consumption of the iron ore sintering process generally accounts for about 10% of iron and steel enterprises, 75%~80% of which are consumed in the form of solid fossil fuels like coke breeze or anthracite [1, 2]. Fuel cost accounts for 40% or more of the sinter processing costs [3]. Also, previous research found that the combustion of solid fossil fuels served as the main source of CO₂, SO_x, NO_x, and so on in this process [4, 5]. To address these problems, substituting extensively distributed, renewable, and clean biochar for fossil fuels in sintering process was believed to be a promising strategy to reduce the emissions of CO₂, SO_x, NO_x, and so on [6–10].

CSIRO in Australia conducted a study on the application of charcoal in iron ore sintering process. The results showed that the ash content of charcoal produced by red eucalyptus was low and the residual impurities were few after burning. When applied to sintering process, the biochar could replace part of the coke breeze but reduced the strength of the sinter product. In particular, the tumble strength was reduced significantly when biochar dosage was high [11, 12]. The

British and Dutch scholars of the Corus Technology and Development Research Center jointly conducted a series of sintering tests which used the sunflower seed shells to replace part of the coke breeze. The results showed that it was feasible to use sunflower seed shell to replace 10% coke breeze in iron ore sintering. The sintering characteristics were similar to the ones when using coke breeze only, while the sintering time shortened and the productivity was improved by 6.4%. However, when the substitution ratio was 20% or higher, the sintering production and quality indicators deteriorated seriously [13, 14]. Brazil research institutions used biochar powder with grain size of 5–10 mm to replace 6% and 12% coke breeze for sintering production, finding that sinter products with the large specific surface area and good metallurgical performance were obtained, and the products could meet the requirements of blast furnace although the tumble strength reduced [15]. Liming LU from CSIRO found that, compared with the sinter fired with coke breeze, the sinter from the mixtures with ≤50% coke powder replaced by charcoal was marginally weaker in terms of sinter yield, tumble strength, and reduction disintegration [16, 17]. Our

TABLE 1: Chemical compositions of raw materials and their proportions in mixture.

Types of raw materials	Chemical composition/wt-%							*Percent/wt-%
	TFe	FeO	SiO ₂	CaO	MgO	Al ₂ O ₃	LOI	
Iron ores blend	63.02	6.50	4.58	0.35	0.28	1.42	3.10	60.73
Dolomite	0.21	0.13	0.71	32.64	19.83	0.56	46.47	5.58
Limestone	0.14	0.10	1.49	50.66	2.28	0.43	40.72	2.16
Quicklime	0.4	0.23	2.86	76.69	1.18	1.20	12.36	4.62
Return fines	56.81	6.25	5.11	9.02	1.86	2.00	0.00	23.08

*The ratio was calculated when the proportion of coke was 3.85%.

TABLE 2: Ultimate and proximate analyses of solid fuels.

Fuel types	Ultimate analyses/wt-%			Proximate analyses (dry base)/wt-%			Calorific value/MJ·kg ⁻¹
	C _{total}	S	N	Fixed carbon	Ash	volatile	
Coke breeze	78.89	0.500	0.72	74.68	19.54	5.88	26.84
Biochar	94.64	0.037	0.19	87.34	5.10	7.55	30.77

group also did a lot of work on the influences of biochar replacing coke breeze on sintering process. The research showed that it could reduce emissions of NO_x, SO_x, and so on when applying the carbonized products of straw, trees, and molded-sawdust [18–21].

There were lots of differences between biochar and conventional fuels in terms of chemical composition, physical properties, proximate analysis, and so on. Biochar replacing coke breeze would bring a series of changes to the behavior of the fuel in sintering process. Therefore, in this paper the differences between biochar and coke breeze in reactivity were studied, as well as the kinetic characteristics of biochar reacting with CO₂. In addition, the mechanism how biochar replacing coke breeze affected the yield and quality of sinter was revealed by researching the influences of biochar on combustion efficiency.

2. Materials and Methods

2.1. Raw Materials. Iron ore blend, solid fuels, fluxes (dolomite, limestone, and quicklime), and return fines were utilized to produce sinter. The chemical compositions of raw materials are shown in Table 1. Several kinds of iron ores were blended to satisfy the requirement of sinter compositions, with TFe (total iron content) of 57.5%, SiO₂ of 4.8% in sinter. Fluxes had the conventional compositions, and their percentages in mixture were calculated to meet basicity (CaO/SiO₂) of 2.0 and MgO of 2.0%.

Two types of solid fuels were applied in the experiments. One was coke breeze, which came from an industrial sintering plant, and the other was biochar carbonized from acutissima at 700 °C for 30 min in nitrogen gas. Ultimate and proximate analyses of fuels are illustrated in Table 2. The chemical compositions of ash in fuels are shown in Figure 1. It can be seen that biochar had lower N and S contents, which was advantageous to reduce the generation of SO_x and NO_x. Compared with coke breeze, biochar was lower in ash content, but higher in fixed carbon, volatile, and calorific value.

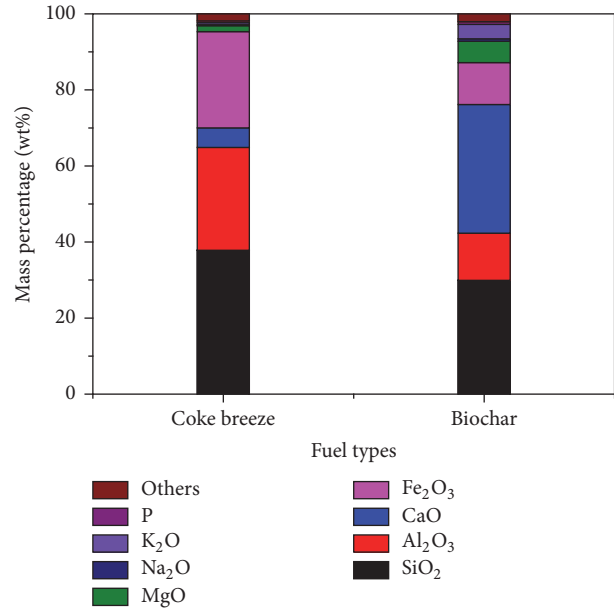


FIGURE 1: Chemical compositions of ash in fuels.

With the help of optical microscope, microstructures of coke breeze and biochar were obtained, as shown in Figure 2. Apparently, more microspores were distributed uniformly inside biochar and the majority of which were microscope. Porosity of biochar and coke breeze was measured by optical microscope, while specific surface areas were tested by Quantachrome Quadra Win. The biochar used in this paper was without activation, so nitrogen was used as adsorbate and BET method was used to calculate specific surface area. The porosity of biochar was 58.22%, which was higher than that of the coke breeze by 12.47%. The specific surface area of biochar was 54.76 m²/g, which was 9.13 times bigger than that of coke breeze.

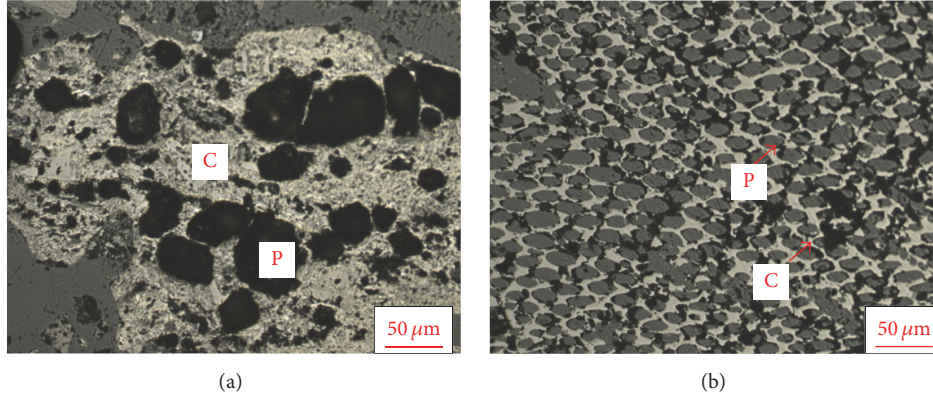


FIGURE 2: Microstructure of solid fuels: (a) coke breeze; (b) biochar; C: carbon; P: pore.

2.2. Methods

2.2.1. Methods to Research Gasification Reaction Behavior. The reactivity of biochar under the nonisothermal condition was studied using the synchronous heat analyzer (NET-ZSCH STA 449C, German). 5.0 mg sample was put in the Al_2O_3 crucible of the thermobalance stent and heated by controlled computer process. The gas flow velocity was controlled, 0.5 m/s, and the speed of temperature increasing was $15^\circ\text{C}/\text{min}$. The TG-DTG curve and DSC curve of gasification reaction between the biochar and CO_2 were analyzed to obtain the characteristic parameters of gasification reaction, including reactions starting temperature (T_s), the end temperature (T_e), the maximum weight loss rate (V_{max}), and the maximum heat release (Q_{max}).

The reactivity of the biochar under isothermal conditions was studied in a vertical furnace. Using a fused silica tube with $\Phi 38 \times 550$ mm as reaction tank, there was a cup for placing sample, which charged by 25 g dried fuel with a size fraction of 3 mm. The weight was measured and recorded by electronic balance and computer, respectively, and the system read the data every 20 s. Before starting the test, nitrogen as protective gas with flow rate of 5 L/min was passed into the tube until the temperature reached the preset temperature again. Then, the reaction tank was weighed and the nitrogen gas was cut off. Then inlet CO_2 with the flow rate of 10 L/min until the weight loss reached a constant value. Thus the gasification reaction conversion rate (x_c) and the instantaneous rate R at a certain time were calculated according to the weight loss value of each time. The formulas are as follows:

$$x_c = \left(1 - \frac{m}{m_0}\right) \times 100\% \quad (1)$$

$$R = -\frac{1}{m_0} \frac{dm}{dt},$$

where x_c is conversion rate, %; R is reaction rate, %/min; m_0 is initial mass, g; m is the mass of reaction of the time t , g; dm/dt is weight loss rate at reaction of the time t , g/min.

The rate of gasification reaction was evaluated using the instantaneous rate $R_{1/2}$ at a fuel conversion of 50%.

2.2.2. Sintering Trials. Sintering process was simulated in a sinter pot of 180 mm diameter \times 700 mm deep. The procedure involved ore proportioning, blending, granulation, ignition, sintering, and cooling. Raw materials were granulated in a drum of 600 mm diameter \times 1400 mm deep for 4 min and then charged into the sinter pot. A hearth layer approximately 20 mm thick was used to protect the grate from thermal erosion. After charging, the fuel in the surface layer was ignited at $1150 \pm 50^\circ\text{C}$ for 1 min by an ignition hood. The combustion front moved downwards with the support of a downdraught system with a negative pressure of 10 kpa. In the sintering process, an infrared analyzer was used to detect the CO and CO_2 contents in exhaust gas, and combustion efficiency of $\text{CO}_2/(\text{CO} + \text{CO}_2)$ was calculated to assess the burning degree of fuels. After sinter cake discharging, dropping test (2 m \times 3 times), screening, and tumble strength were carried out to evaluate the physical strength of sinter. Yield was the proportion of product sinter which deducted the hearth layer material and the fines -5 mm. Productivity was defined as the weight of product sinter produced per area per time. The test of tumble strength was conducted in a drum of $\Phi 1000 \times 500$ mm where 7.5 kg product sinter was tumbled for 200r, then tumbled sinter was screened at 6.3 mm, and the proportion of $+6.3$ mm was treated as tumble strength. Sintering speed was the ratio between the height of sintering bed and the total sintering time.

During the sinter pot tests, the mass of biochar was calculated on the basis of replacement percentage biochar replacing coke and the heat replacement ratio by

$$m_b \cdot h_b \cdot a = m_c \cdot h_c \cdot r, \quad (2)$$

where m_b is the mass of biochar, kg; m_c is the mass of coke for the base case, kg; r is the percentage of biochar replacing coke, which means the reduction percentage of coke compared to the base case as biochar replacing coke; h_c is the calorific value of coke, $\text{MJ}\cdot\text{kg}^{-1}$; h_b is the calorific value of biochar, $\text{MJ}\cdot\text{kg}^{-1}$; a is the heat replacement ratio, which means that 1 kJ heat released by biochar can replace the amount of heat released by coke; as $a = 1$, it means that the heat of biochar combustion was equivalent to that for the coke breeze substituted.

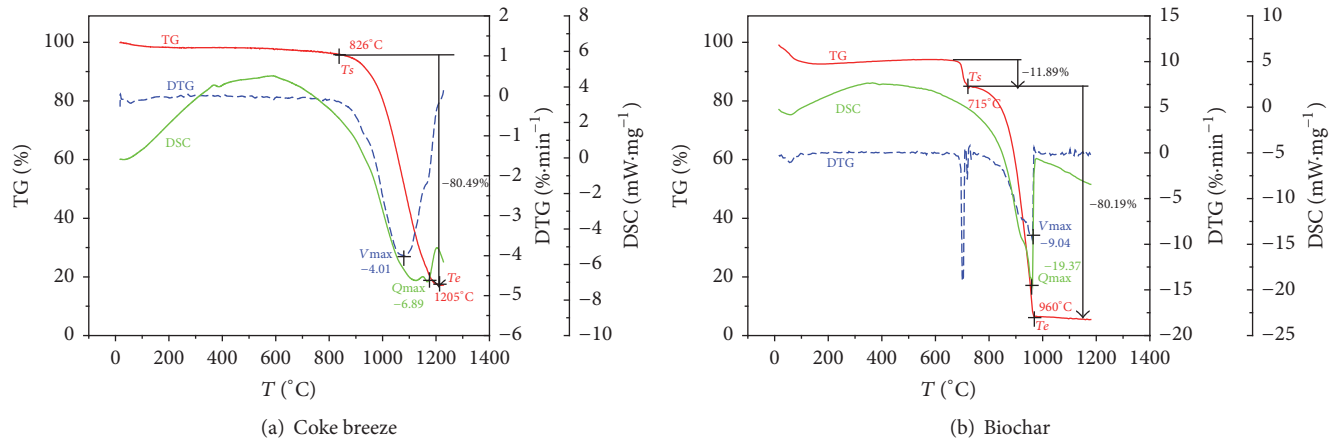


FIGURE 3: TG-DSC curves of nonisothermal gasification of fuels.

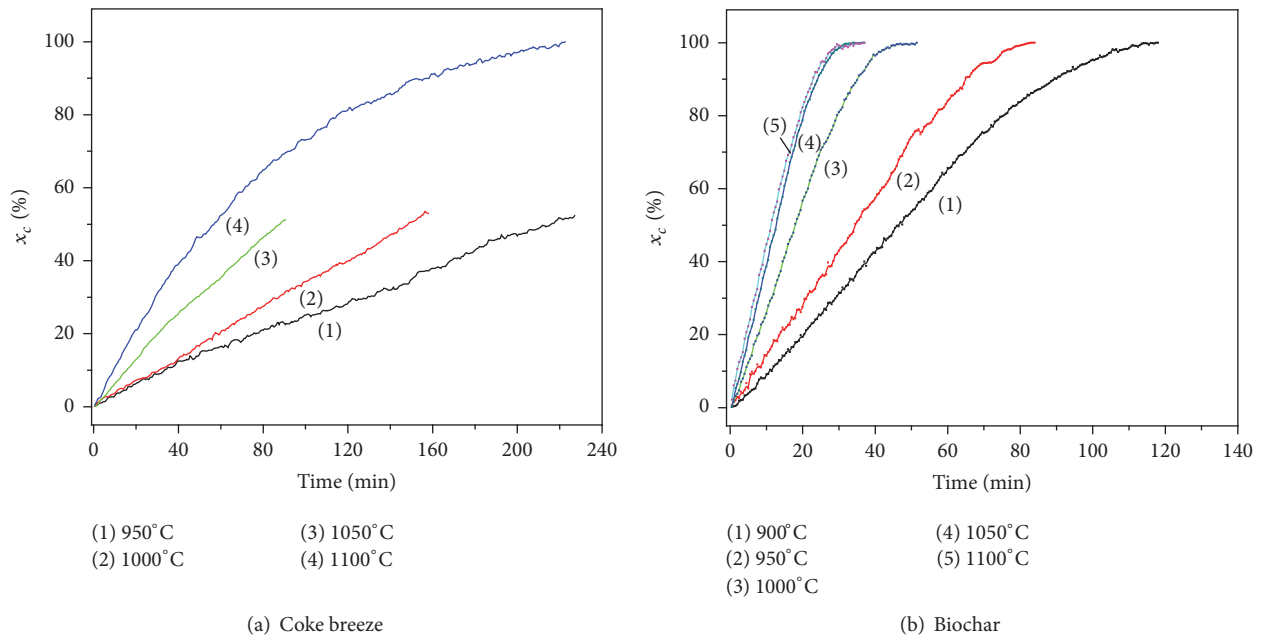


FIGURE 4: Effect of temperature on gasification of fuels.

3. Results and Discussion

3.1. Thermochemical Behavior of Biochar

3.1.1. Gasification Characteristic Parameters. The TG-DSC curves of nonisothermal gasification of fuels are shown in Figure 3. Biochar heated in CO_2 atmosphere went through four stages, which were drying, warming up, volatiles desorption, and gasification reaction of carbon, respectively. Volatile began to separate out when the temperature reached a certain value, compared with coke breeze, the weight loss of biochar during which process was more obvious and the volatile weight loss ratio could normally reach more than 8%. After the desorption of volatile, it came to the gasification of fixed carbon, and the weight loss ratio of fuel sped up significantly. The DTG and DSC curves of biochar showed sharp peaks,

indicating that the reaction was more intense compared with coke breeze.

The TG-DTG and DSC curves of fuels' gasification were analyzed to obtain the characteristic parameters. It showed that biochar started to gasify at low temperature, and the reaction starting temperature (T_s) and the end temperature (T_e) were both lower than those of the coke breeze, while the maximum weight loss rate (V_{\max}) and maximum heat absorption value (Q_{\max}) were both higher than those of the coke breeze. It manifested that biochar had a higher reactivity than coke breeze and easily reacted with CO_2 to generate CO .

3.1.2. Gasification Dynamics. The reaction rates of biochar and coke breeze with CO_2 were studied by isothermal thermogravimetric analysis and the conversion rates are shown in Figure 4. For comparing the gasification process between

TABLE 3: Activation energy of fuel gasification and the transition temperature of every zone.

Fuel	Activation energy/kJ·mol ⁻¹			Transition temperature/°C	
	Chemical reaction	Internal diffusion	External diffusion	Chemical reaction → internal diffusion	Internal diffusion → external diffusion
Coke breeze	187.36	77.16	33.51	950	1100
Biochar	131.10	71.82	31.88	900	1000

fuel and CO₂, the rate of gasification reaction was evaluated by the instantaneous speed ($R_{1/2}$) when the conversion rate was 50%. It was known from Figure 3 that, at the same temperature, the gasification reaction rate of the biochar was 3.85%/min, which was faster than that of the coke breeze (0.57%/min) at 1050°C. With temperatures rising, gasification reaction speed of fuel got faster, which shortened the time during which fuel conversion rate reached 50%. When the temperature ranged from 950°C to 1100°C, the gasification reaction rate ($R_{1/2}$) of biochar increased from 1.50%/min to 4.35%/min, and $t_{1/2}$ decreased from 34.33 min to 11.52 min.

In this paper, a typical shrinking core reaction model was used to study the gasification reaction kinetics of solid fuels. The reaction can be divided into three zones: chemical reaction kinetics zone, inner diffusion zone, and outer diffusion zone. In the chemical reaction kinetics zone, the controlling factor of the reaction rate is the chemical reaction of coke and CO₂. In the outer diffusion zone, the controlling factor is the effect of CO₂ diffusing to coke surface, while the internal diffusion zone is affected by both chemical reaction and diffusion. Tseng and Edgar [22] analyzed the different reaction zones of coke. In the chemical reaction kinetics zone, the kinetic constant of coke gasification reaction is expressed by the following formula:

$$k_v = \frac{1}{P_{O_2} t_{1/2} S_0} \int_0^{0.5} \frac{S_0}{S} dx_c. \quad (3)$$

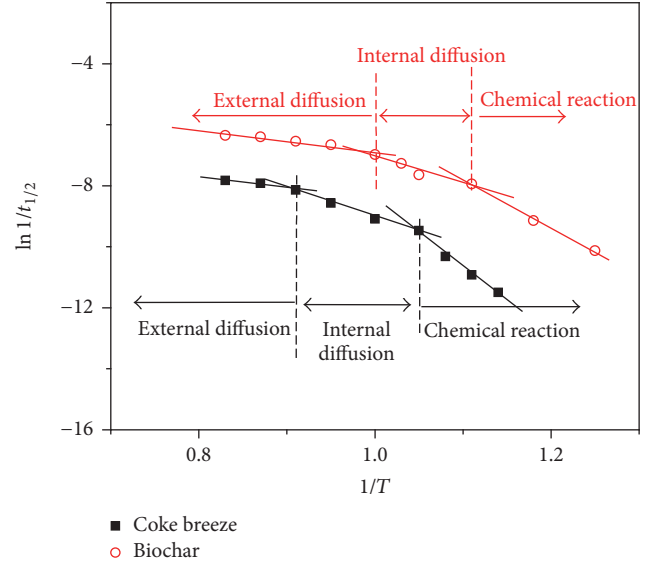
The internal diffusion rate constant of coke gasification in the internal diffusion zone is described in the following formula:

$$k_s = \frac{r_0}{P_{O_2} a t_{1/2}} \left(1 - \sqrt[3]{\frac{1}{2}} \right). \quad (4)$$

In the outer diffusion zone, the external diffusion rate constant of coke gasification is represented by the following formula:

$$S_h = \frac{(1 - x_a) \rho_p r_0^2 RT}{D_b \omega P_{O_2} t_{1/2}} \left(1 - \sqrt[3]{\frac{1}{4}} \right). \quad (5)$$

In the formula, k_v is gasification rate constant; k_s is the internal diffusion rate constant; S_h is the outer diffusion rate constant; x_c is coke conversion rate; $t_{1/2}$ is the reaction time when the conversion rate reached 50%; S is specific surface area at any time during gasification process; P_{O_2} is the oxygen partial pressure; n is intrinsic reaction order; a is apparent reaction order; r_0 is initial particle radius of coke; D_b is diffusion coefficient of CO₂; x_a is ash ratio; ω is the amount of carbon consumed per mole of CO₂; R is gas constant.

FIGURE 5: Relationship between $\ln 1/t_{1/2}$ and $1/T$ of fuel gasification.

The reaction rate constant $k(T)$ can be represented by the Arrhenius formula

$$k(T) = k_0 \exp\left(-\frac{E}{RT}\right). \quad (6)$$

Combining the above equations, the following formula (7) can be obtained:

$$\ln \frac{1}{t_{1/2}} = \ln \frac{k_0}{C} - \frac{E}{RT}. \quad (7)$$

The activation energy E of gasification can be obtained by the slope of $\ln 1/t_{1/2}$ and $1/T$. The change curve of $\ln 1/t_{1/2}$ of biochar and coke breeze with the change of $1/T$ was shown in Figure 5, and the activation energy and transition temperature were shown in Table 3.

It was shown in Table 3 that when the gasification reaction was in the external diffusion and internal diffusion control zone, the activation energy of biochar's gasification was slightly smaller than that of coke breeze, while, in the control of the chemical reaction zone, the activation energy of biochar's gasification was significantly lower than that of coke breeze. The activation energy of biochar's gasification was 131.10 kJ/mol, which was lower than that of coke breeze by 56.26 kJ/mol. Biochar's gasification transferred from chemical reaction control to internal diffusion control at 900°C, while transferring from internal diffusion control to external diffusion at 1000°C. Obviously, the transition temperature was lower than that of the coke breeze.

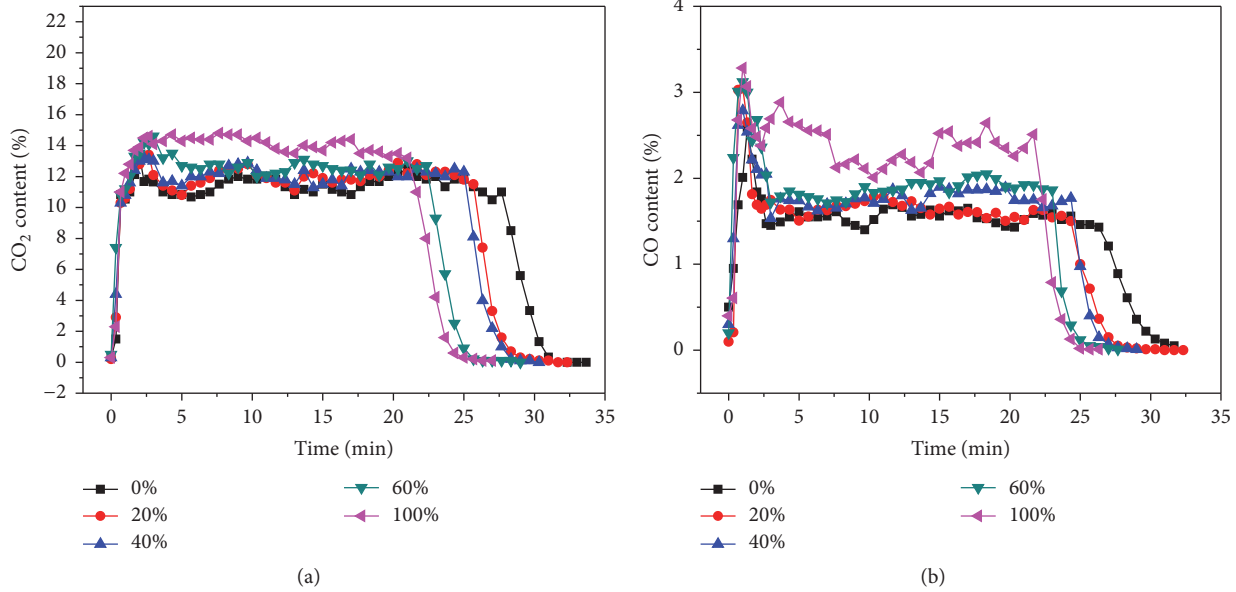


FIGURE 6: Effect of proportion of biochar replacing coke on CO_x concentrate of flue gas.

3.2. *The Effect of Biochar on Sintering.* The effect of proportion of biochar replacing coke at equal heat substitution on sintering process was studied. The effect of biochar replacing coke breeze on the emission of CO₂ and CO during sintering was shown in Figure 6. With the increase of substitute proportion, the content of CO₂ and CO in flue gas increased. More fuel was burned per unit time due to the increasing of burning speed when using biochar in sintering. When the substitute proportion increased from 0% to 100%, the average concentration of CO₂ and CO in flue gas increased from 10.32% and 1.43% to 12.27% and 2.14%, respectively.

Combustion efficiency refers to the ratio of complete combustion to the whole combustion. The ratio of CO₂/(CO + CO₂) can reflect the combustion efficiency. When C is combust at high temperature, the reaction on the surface of C is the gasification reaction between C and CO₂, and the produced CO diffuses outward and reacts with O₂ diffusing inward to generate CO₂. Therefore, combustion efficiency was affected by the rate of CO₂ + C = 2CO reaction on the surface of carbon particle. The influences of biochar replacing coke breeze on combustion efficiency were illustrated in Figure 7. Evidently, combustion efficiency was decreased with the increase of biochar ratios, and when they were 20%, 40%, 60%, and 100%, the average combustion efficiency was decreased from 87.83% to 87.82%, 86.92%, 86.04%, and 85.15%, respectively, which indicated that incomplete combustion developed with the increase of biochar ratios in sintering process. The heat released by the combustion of carbon was just 29.25% of its total calorific value when it combusted incompletely, which meant a high heat loss portion of 70.75%. Therefore, biochar replacing coke breeze would lower the efficiency of heat utilization.

From the above, it is known that biochar was characterized by higher reactivity than coke breeze and could react with CO₂ rapidly. Therefore, more CO was generated

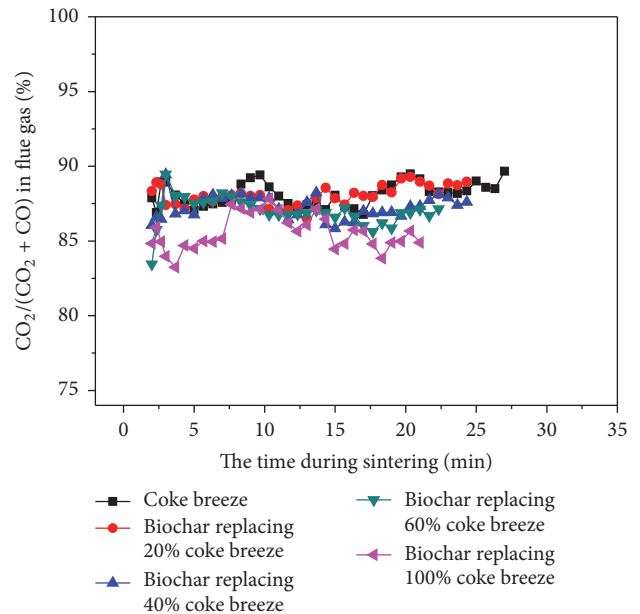


FIGURE 7: Influence of biochar replacing coke breeze on combustion efficiency.

on the surface of biochar. Furthermore, as biochar burned quickly, more O₂ was consumed per unit time and the concentration of O₂ in flue gas was relatively low, which limited the secondary combustion reaction of CO and finally made combustion efficiency drop, which finally decreased the production and quality index of sintering.

The effect of biochar replacing coke breeze at equal heat substitution on the yield and quality of sinter was shown in Table 4. With the increase of substitute proportion, the sintering speed accelerated, while the sinter yield, tumble

TABLE 4: Effect of biochar replacing coke breeze on sintering indexes.

Biochar replacing coke ratio/%	Suitable moisture/%	Sintering speed/mm·min ⁻¹	Yield/%	Tumble strength/%	Productivity/t·m ⁻² ·h ⁻¹
0	7.25	21.94	72.66	65.00	1.48
20	7.25	24.58	68.69	64.40	1.52
40	7.50	24.73	65.30	63.27	1.43
60	7.50	27.20	55.35	54.67	1.32
100	7.75	27.17	41.11	23.87	0.93

TABLE 5: Effect of heat replacement ratio on sintering indexes.

Heat replacement ratio	Sintering speed/mm·min ⁻¹	Yield/%	Tumble strength/%	Productivity/t·m ⁻² ·h ⁻¹
1.00	24.73	65.30	63.27	1.43
0.85	24.29	67.27	64.47	1.41
0.75	23.88	69.63	64.18	1.46

strength, and productivity decreased. When the substitute proportion of biochar was relatively low, the decreasing extent was not significant. However, when the substitute proportion exceeded a certain value, the sinter yield and quality index deteriorated greatly. Therefore, the proportion of biochar replacing coke breeze had an appropriate value. When the substitute proportion was more than 40%, the sinter yield and quality index dropped rapidly, indicating that the appropriate substitute proportion was 40%.

The main reason why sinter yield and tumble strength decreased was that the biochar burnt too fast, causing the deterioration of combustion efficiency and the drop of bed layer temperature. Consequently, reducing the heat replacement ratio of biochar for raising the temperature of bed layer could improve the yield and tumble strength of sinter. The effect of heat replacement ratio on sintering indexes was shown in Table 5. When the ratio of the heat released by biochar replacing that for the coke reduced from 1.00 to 0.75, the yield of sinter increased from 65.30% to 69.63%, and the tumble strength increased from 63.27% to 64.18%. Therefore, reducing the heat replacement ratio of biochar could improve the yield and quality of sinter.

4. Conclusion

- (1) The initial temperature and the final temperature of the gasification reaction between biochar and CO₂ were low, the speed was fast, and the maximum weight loss rate and heat absorption were both higher than those of the coke breeze. Dynamic parameters showed that the gasification activation energy of biochar was 56.26 kJ/mol, lower than coke breeze, which indicated that the biochar had better reactive activity.
- (2) Due to biochar's high reactivity, the degree of incomplete combustion in the sintering process increased and the thermal efficiency reduced, which was not conducive to the high-temperature mineralization process. As a result, the sinter yield, tumble strength, and productivity decreased with the increase of

biochar's substitute proportion. Therefore, the proportion of biochar replacement of coke breeze at equal heat substitution should be controlled no more than 40%. Reducing the heat replacement ratio of biochar could improve the temperature of sinter bed, improving the yield and tumble strength of sinter.

Conflicts of Interest

The authors declare that they have no conflicts of interest.

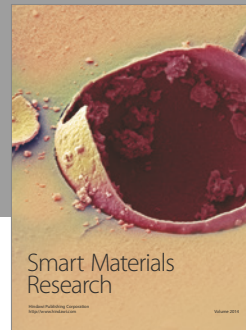
Acknowledgments

The research was financially supported by the State Key Program of National Natural Science Foundation of China (no. U1660206), Natural Science Foundation of Hunan Province in China (no. 2015JJ3164), Hunan Provincial Co-Innovation Center for Clean and Efficient Utilization of Strategic Metal Mineral Resources and Innovation Driven Plan of Central South University (no. 2015CX005), Hunan Provincial Innovation Foundation for Postgraduate (CX2016B054), and Open-End Fund for the Valuable and Precision Instruments of Central South University (CSUZC201703).

References

- [1] Z. Z. Hao, S. L. Wu, and X. G. Duan, "Practice of reducing sintering process energy consumption in Baosteel," *Sintering Pelletizing*, vol. 35, article 46, 2010.
- [2] S. Q. Li, Z. J. Ji, L. Wu et al., "An analysis on the energy consumption of steel plants and energy-saving measures," *Industrial Heating*, vol. 39, no. 5, pp. 1–3, 2010.
- [3] X. M. Liang, D. Q. Zhu, T. Jiang et al., "Present State of Sintering Energy Saving Techniques and Prospect," *Sintering and Pelletizing*, vol. 25, no. 4, pp. 1–4, 2000.
- [4] Y. G. Chen, Z. C. Guo, Z. Wang, and G. S. Feng, "NO_x reduction in the sintering process," *International Journal of Minerals, Metallurgy and Materials*, vol. 16, no. 2, pp. 143–148, 2009.

- [5] Y. Chen, Z. Guo, and Z. Wang, "Influence of CeO₂ on NO_x emission during iron ore sintering," *Fuel Processing Technology*, vol. 90, no. 7-8, pp. 933–938, 2009.
- [6] P.-A. Glaude, R. Fournet, R. Bounaceur, and M. Molière, "Adiabatic flame temperature from biofuels and fossil fuels and derived effect on NO_x emissions," *Fuel Processing Technology*, vol. 91, no. 2, pp. 229–235, 2010.
- [7] J. Liu, G. Zhai, and R. Chen, "Analysis on the characteristics of biomass fuel direct combustion process," *Journal of Northeast Agricultural University*, vol. 3, pp. 290–294, 2001.
- [8] C. Bartolomé and A. Gil, "Emissions during co-firing of two energy crops in a PF pilot plant: Cynara and poplar," *Fuel Processing Technology*, vol. 113, pp. 75–83, 2013.
- [9] H. Spliethoff and K. R. G. Hein, "Effect of co-combustion of biomass on emissions in pulverized fuel furnaces," *Fuel Processing Technology*, vol. 54, no. 1-3, pp. 189–205, 1998.
- [10] R. C. Guo, J. R. Tang, H. Xu, and H. C. Ma, "The status and vision for utilization of lignified biomass energy," *Forest Inventory & Planning*, vol. 32, no. 1, pp. 90–94, 2007.
- [11] R. Lovel, K. Vining, and M. Dell'Amico, "Iron ore sintering with charcoal," *Transactions of the Institutions of Mining and Metallurgy, Section C: Mineral Processing and Extractive Metallurgy*, vol. 116, no. 2, pp. 85–92, 2007.
- [12] M. Zandi, M. Martinez-Pacheco, and T. A. T. Fray, "Biomass for iron ore sintering," *Minerals Engineering*, vol. 23, no. 14, pp. 1139–1145, 2010.
- [13] T. C. Ooi, E. Aries, B. C. R. Ewan et al., "The study of sunflower seed husks as a fuel in the iron ore sintering process," *Minerals Engineering*, vol. 21, no. 2, pp. 167–177, 2008.
- [14] S. N. Silva, F. Vernilli, D. G. Pinatti et al., "Behaviour of biofuel addition on metallurgical properties of sinter," *Ironmaking and Steelmaking*, vol. 36, no. 5, pp. 333–340, 2009.
- [15] H. Helle, M. Helle, H. Saxén, and P. Frank, "Mathematical optimization of ironmaking with biomass as auxiliary reductant in the blast furnace," *ISIJ International*, vol. 49, no. 9, pp. 1316–1324, 2009.
- [16] L. Lu, M. Adam, M. Kilburn et al., "Substitution of charcoal for coke breeze in iron ore sintering," *ISIJ International*, vol. 53, no. 9, pp. 1607–1616, 2013.
- [17] L. Lu, M. Adam, M. Somerville, S. Hapugoda, S. Jahanshahi, and J. G. Mathieson, "Iron ore sintering with charcoal," in *Proceedings of the 6th Int. Cong. of the Science and Technology of Ironmaking – ICSTI 2012*, Brazilian Association for Metallurgy, Materials and Mining, Rio de Janeiro, Brazil, 2012.
- [18] M. Gan, X. Fan, X. Chen et al., "Reduction of pollutant emission in iron ore sintering process by applying biomass fuels," *ISIJ International*, vol. 52, no. 9, pp. 1574–1578, 2012.
- [19] X. Fan, Z. Ji, M. Gan, X. Chen, Q. Li, and T. Jiang, "Influence of charcoal replacing coke on microstructure and reduction properties of iron ore sinter," *Ironmaking and Steelmaking*, vol. 43, no. 1, pp. 5–10, 2016.
- [20] X. Fan, Z. Ji, M. Gan, X. Chen, L. Yin, and T. Jiang, "Preparation technologies of straw char and its effect on pollutants emission reduction in iron ore sintering," *ISIJ International*, vol. 54, no. 12, pp. 2697–2703, 2014.
- [21] M. Gan, X. Fan, Z. Ji, X. Chen, T. Jiang, and Z. Yu, "Effect of distribution of biomass fuel in granules on iron ore sintering and NO_x emission," *Ironmaking and Steelmaking*, vol. 41, no. 6, pp. 430–434, 2014.
- [22] H. P. Tseng and T. F. Edgar, "Identification of the combustion behaviour of lignite char between 350 and 900 °C," *Fuel*, vol. 63, no. 3, pp. 385–393, 1984.



Hindawi

Submit your manuscripts at
<https://www.hindawi.com>

